Journal Pre-proof

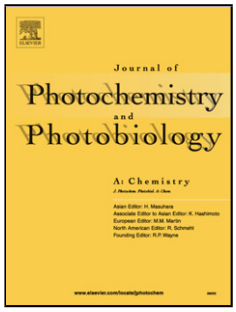

UV laser induced photolysis of glycolic acid isolated in argon matrices

Justyna Krupa (Investigation) (Visualization) (Writing - review and editing), Iwona Kosendiak (Investigation), Maria Wierzejewska (Conceptualization) (Writing - original draft), Jussi Ahokas (Investigation), Jan Lundell (Conceptualization)

PII: S1010-6030(21)00108-8

DOI: https://doi.org/10.1016/j.jphotochem.2021.113236

Reference: JPC 113236

To appear in: *Journal of Photochemistry & Photobiology, A: Chemistry*

Received Date: 28 October 2020

Revised Date: 26 February 2021

Accepted Date: 27 February 2021

Please cite this article as: Krupa J, Kosendiak I, Wierzejewska M, Ahokas J, Lundell J, UV laser induced photolysis of glycolic acid isolated in argon matrices, *Journal of Photochemistry and amp; Photobiology, A: Chemistry* (2021), doi: https://doi.org/10.1016/j.jphotochem.2021.113236

UV laser induced photolysis of glycolic acid isolated in argon matrices

Justyna Krupa[1], Iwona Kosendiak[1], Maria Wierzejewska[1*], Jussi Ahokas[2], Jan Lundell[3*]

[1]Faculty of Chemistry, University of Wrocław, Joliot-Curie 14, 50-383 Wrocław, Poland

[2]Department of Chemistry and Nanoscience Center, University of Jyväskylä, FI-40014 Jyväskylä, Finland

[3]Department of Chemistry, University of Jyväskylä, FI-40014 Jyväskylä, Finland

Graphical abstract

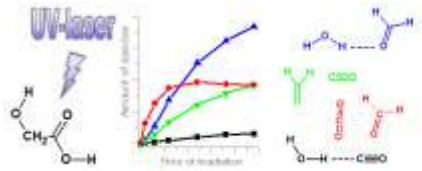

Highlights

- UV-laser induced photolysis of glycolic acid in solid Ar studied for the first time
- Complexes formed between photoproducts: HCHO, H_2O, CO and CO_2 identified by FTIR
- Composition and structure of complexes determined by quantum-chemical calculations
- Amount of complexes depends on interaction energy and arrangement of photoproducts

Abstract

The photochemistry of matrix-isolated glycolic acid, induced by UV light, was studied by FTIR spectroscopy and B3LYPD3/6-311++G(3df,3pd) calculations. Several decomposition pathways were found to take place upon 212 nm and 226 nm wavelengths irradiation. A number of complexes formed between photoproducts were identified, among them those of formaldehyde with water, carbon monoxide and carbon dioxide as well as the H_2O-CO complexes. The structure and spectroscopic assignment of the photoproducts were made comparing the experimental results with the theoretical predictions and available literature data. The observed formation of different complexes indicates various pathways for their formation resulting from UV-induced photodecomposition of different precursor isomers.

Keywords: molecular complexes; vibrational spectroscopy; Matrix isolation; carboxylic acid; computational chemistry

1. Introduction

Glycolic acid (GA), the simplest representative of the hydroxyacids, has been the subject of numerous studies both in the gas phase [1-234] and in low temperature matrices [5-6789]. In a free jet expansion study only the most stable SSC conformer was detected by microwave spectroscopy along with a small amount of the AAT form [1]. SSC is also the dominant

conformer in freshly deposited low temperature matrices with small quantity of two less stable GAC and AAT species. The three most stable GA conformers are shown in Scheme 1. The experimental characterization and possible interconversions between different forms of glycolic acid have been most frequently studied using FTIR spectroscopy coupled with matrix isolation technique. A number of these studies deal with the analysis of possible interconversions between the GA forms induced by selective first overtone excitation of the νOH mode [6-8]. Very recently it was demonstrated that selective conformational isomerisations also take place using excitation of second OH stretching overtones [10]. In turn, the high vibrational overtone-induced isomerisations of GA were observed using Raman spectroscopy and photo-induced equilibrium between the three most stable conformers was detected [9]. Suhm *et al.* have recently shown that glycolic acid represents a well-suited example to be used as a vibrational anharmonicity benchmark [11].

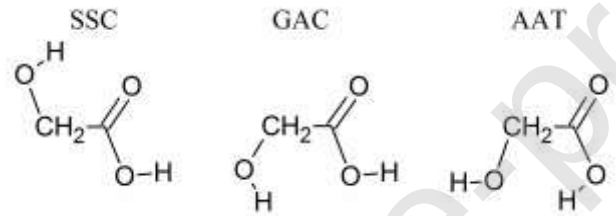

Scheme 1. Schematic representation of three most stable conformers of glycolic acid monomer.

Since glycolic acid contains two OH groups, it is capable to form both intra- and intermolecular hydrogen bonds. Therefore, GA can serve as a model compound to understand how the two competing hydroxyl groups influence ability of a molecule to form molecular complexes. The interaction of glycolic acid with N_2 as well as structural changes of GA-N_2 induced by selective overtone vibrational excitation of the νOH mode were studied in argon matrices using FTIR [12,13] and Raman spectroscopy [14]. FTIR matrix isolation and theoretical studies on glycolic acid dimers were also reported [15].

This work presents results of the UV photolysis of glycolic acid upon the monochromatic radiation from a tunable light source. Previously, such studies have not yet been carried out for glycolic acid, which impose interesting questions for the difference in photochemical processes when photolysis wavelengths are changed from IR and visible light photons to UV-photons. Here, as the main experimental approach, matrix isolation technique was used combined with FTIR spectroscopy, which guarantees the high-intrinsic spectral resolution necessary for the identification and characterization of photoproducts. Interpretation of the experimental results obtained in the present study was supported by quantum chemical calculations performed at the B3LYPD3/6-311++G(3df,3pd) level of theory to ensure similar theoretical treatment for emerging photoproducts.

2. Experimental

The GA/Ar matrices were prepared by passing of high purity argon (Messer, 5.0) through the glass U-tube with GA (Janssen Chimica, purity 99%) kept at room temperature and situated outside the cryostat chamber. Due to the way of deposition, the matrix-to-sample ratio could not be precisely determined. Matrices containing monomeric GA species were obtained by applying the matrix deposition temperature of 15 K and the gas flow rate of 2.5 mbar per minute. Such experimental conditions were chosen based on the previous GA dimer studies [15] during which both the deposited acid temperature and the matrix gas flow rate were changed thus affecting the monomer/dimer ratio. The GA/Ar gaseous mixtures were deposited onto a cold CsI window kept at 15 K by a closed cycle helium cryostat APD-Cryogenics (ARS-2HW). Low temperature was monitored by a Scientific Instruments 9700 temperature controller equipped with a silicon diode. FTIR spectra were collected at 10 K in a transmission mode with a 0.5 cm^{-1} resolution using a Bruker IFS 66 Fourier Transform spectrometer equipped with a liquid N_2 cooled MCT detector.

The GA/Ar matrices were irradiated with the UV radiation provided by the frequency doubled signal beam of a pulsed (7 ns, repetition rate of 10 Hz) optical parametric oscillator Vibrant (Opotek Inc.), pumped with a Nd:YAG laser (Quantel). The vertical excitation energy values of the two lowest singlet-singlet transitions of the SSC conformer of GA are equal to 203 nm and 193 nm for $S_0 \rightarrow S_1$ and $S_0 \rightarrow S_2$, respectively. Based on these results and on the experimental UV spectrum of GA [16] and our spectrum obtained for GA in a water solution (Fig. S1 in Supplementary data) we decided to use the 212 nm irradiation wavelength as the most prominent means of irradiation of the glycolic acid precursor. Later on, we performed additionally studies with λ=226 nm which appeared, in agreement with the data in Fig. S1, also sufficient for the SSC photolysis. The average pulse energies were 1.5 mJ and 2.9 mJ at 212 and 226 nm, respectively.

To support the interpretation of the experimental data computational studies were carried out using the Gaussian16 program package [17]. Structures of the putative photoproducts were optimized at the B3LYPD3 [18-19202122] level of theory with the 6–311++G(3df,3pd) [23,24] basis set. Optimization of the complexes was done with the Boys-Bernardi full counterpoise method by Dannenberg [25,26]. Harmonic frequencies and infrared intensities of the species of interest were computed at the same level to assist the analysis of the UV-irradiated infrared spectra and to verify that the computed structures correspond to the minima. The harmonic frequencies were scaled using two factors: 0.9715 and 0.9556 below and above 2500 cm^{-1}, respectively. These scaling factors give the best agreement between predicted and observed

frequencies. The vibrational stick spectra were simulated using VMS-Draw tool [27]. Vertical excitation energies were calculated using time-dependent density functional theory (TD-DFT) [28,29].

3. Results and discussion

There are several possible UV photolysis pathways of GA. One of them may be the decarboxylation process leading to CO_2 and methanol molecules. Domingo *et al.* reported the theoretical study of the gas phase decomposition of GA. They considered three paths, all of them result in formation of H_2O, CO and formaldehyde molecules [30]. Another possible reaction may be formation of CO_2 and HCHO and dihydrogen molecules. For the GA isolated in low temperature matrices one has to expect that each possible set of photoproducts will be formed in one matrix cage. Thus, interaction between the newly formed species has to be considered as well. Therefore, we performed a number of theoretical calculations on photoproducts and their binary and ternary complexes at the B3LYPD3/6-311++G(3df,3pd) level of theory. The obtained theoretical data of these species are shown in Table 1 together with the available experimental results and in Tables S1-S3 in Supplementary data. In addition to the monomeric species, eleven binary complexes have been considered, which are formed between formaldehyde and carbon monoxide, carbon dioxide and water as well as those formed between water and CO and CO_2. Interaction of methanol with carbon dioxide was also taken into account. Five ternary complexes were considered as well. All these computational studies were performed to ensure a similar theoretical treatment for plausible photodecompsition products and their computed vibrational spectra in support of experimental assignment.

Infrared spectrum measured for freshly deposited GA/Ar matrix was consistent with that previously known in the literature showing the most stable SSC conformer present at high concentration together with two less stable AAT and GAC conformers present at much smaller amounts [8]. Thereafter, matrix samples were subjected to UV irradiation from OPO system. Different wavelengths were tested in order to induce different photo-processes in the GA/Ar matrices. The most pronounced changes were observed for irradiation upon 212 nm and these experiments will be described here. Analogous data obtained using the wavelength of 226 nm are shown in Figs S2-S6 in Supplementary data.

A number of new bands, not observed in the spectrum after the GA/Ar matrix deposition, appeared in the spectra upon UV irradiation. Fig. 1 shows water asymmetric, symmetric stretching and deformation regions of the spectra obtained upon 240 min of 212 nm irradiation of the GA/Ar matrices. B3LYPD3/6-311++G(3df,3pd) theoretical stick spectra of

the relevant species are shown at the bottom of the figure. Fragments of the spectra taken upon annealing at 30 K (measured at 10 K) of the irradiated matrices are added as well.

As a result of both irradiation wavelengths used, the intensity of bands of less stable AAT and GAC conformers of glycolic acid increased slightly, whereas those of SSC conformer decreased. This indicates that during UV-photolysis glycolic acid isomerization takes place suggesting that all isomers act as potential photochemical precursors. In the current stage of the work we are not able to determine which photoproducts result from which precursor nor to determine the photoinduced kinetics between various isomers upon UV photolysis. Such prolonged experimental investigations combined with kinetic modelling is outside the scope of this study.

UV irradiated samples of the GA/Ar matrices produced strong vibrational absorptions in H_2O stretching and bending regions. They are situated at 3706.5 with 3703.5 shoulder, 3569.0 and 1609.5 cm^{-1}. New bands were also found close to the formaldehyde modes at 2884.5, 2817.5, 1735.0, 1499.0, 1246.0 and 1173.5 cm^{-1} and some of these bands are presented in Fig. 2. This set of absorptions, denoted with blue triangles in Figs 1 and 2, is very close to that previously reported for formaldehyde complexed to water molecule [31] (see Table 1) and as such is assigned here to the 1:1 HCHO-H_2O complex.

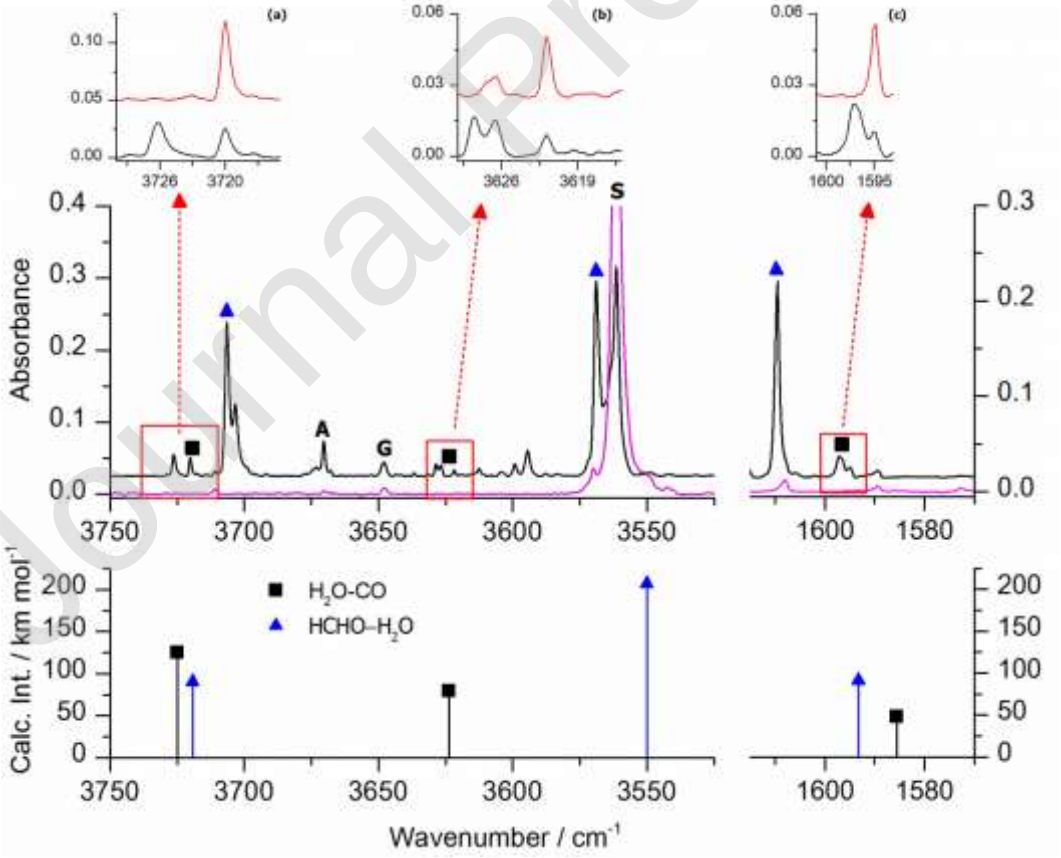

Fig. 1. Water asymmetric and symmetric stretching and deformation regions in the spectra of GA/Ar matrices upon deposition at 15/10K (pink traces) and upon 240 min of irradiation at λ=212 nm (black traces). The insets show behavior of the H_2O-CO doublets upon 10 min annealing at 30 K/10 K (red traces). B3LYPD3/6-311++G(3df,3pd) theoretical stick spectra of HCHO-H_2O and H_2O-CO are shown in the bottom of the figure. Letters A, G and S denote AAT, GAC and SSC conformers of glycolic acid, respectively.

It is worth noting that recently published VUV photolysis of formaldehyde at λ>120 nm proved formation of the HCO radical in low temperature matrices [32]. The infrared bands due to this species in solid argon were found at 2482, 1863 and 1085 cm^{-1}. Inspection of the present GA/Ar spectra upon irradiation at λ=212 nm showed no bands at these wavenumbers. Apparently, the latter wavelength was not sufficient to induce formation of the HCO radicals.

Another set of absorptions due to the perturbed H_2O modes appeared as doublets in the spectra obtained upon irradiation at 3726.0/3720.0 and 1597.0/1595.0 cm^{-1} and as triplet 3628.5, 3626.5/3622.0. As demonstrated in the insets in Fig. 1, one component of each multiplet disappears upon annealing the matrix to 30 K and peaks at 3720.0, 3622.0 (3626.5) and 1595.0 cm^{-1} are left. Simultaneously, as presented in Fig. 3, a doublet is observed in the region of the carbon monoxide fundamental mode at 2151.5/2148.0 cm^{-1} with the latter band remaining upon annealing.

Both position and behavior of the described set of absorptions are consistent with those obtained for the H_2O-CO complex formed in argon matrices upon UV-induced photodecomposition of HCOOH [33,34] and confirm that also in the present case H_2O-CO is formed in different trapping sites. Upon annealing the less stable sites relax to form the lower energy sites, which is demonstrated by decreased number of satellite bands observed.

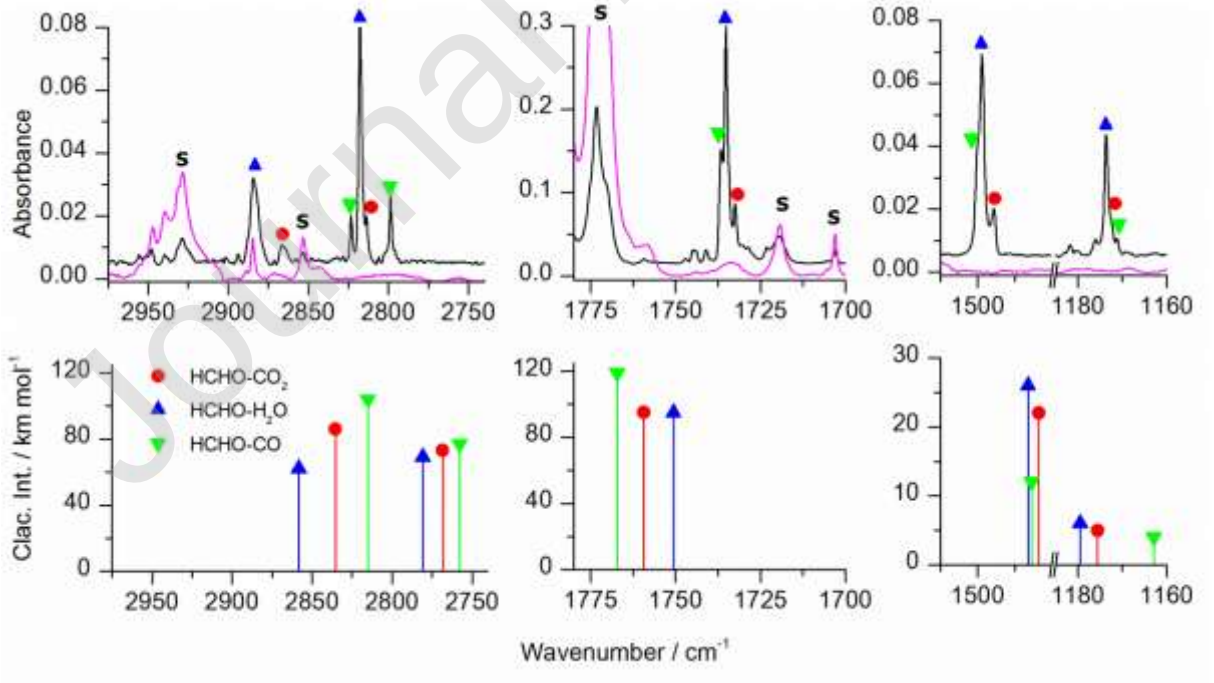

Fig. 2. Selected regions of HCHO complexes with H_2O, CO and CO_2 in the spectra of GA/Ar matrices upon deposition at 15/10K (pink traces) and upon 240 min of irradiation at λ=212 nm (black traces). B3LYPD3/6-311++G(3df,3pd) theoretical stick spectra of the complexes are shown in the bottom of the figure. Letter S denotes SSC conformer of glycolic acid.

As seen in Fig. 3 there are, in addition to those originating from H_2O-CO complex, other new bands appearing upon irradiation in the CO stretching region. They are situated at 2146.0, 2144.5, 2143.0 and 2139.5 cm^{-1}. All of them are shifted to higher wavenumbers compared to the CO monomer band (2138.6 cm^{-1}) [35] with the shifts in the range of 7.4-0.9 cm^{-1}, and indicating a hydrogen bonded complex from the carbon end of CO [33]. The band at 2139.5 cm^{-1} that is the least shifted compared to the monomer CO band position may be assigned with confidence to the monomeric carbon monoxide.

Table 1. Calculated and scaled harmonic wavenumbers ν (cm^{-1}), intensities I (km mol^{-1}) and shifts relative to the corresponding monomers Δν (cm^{-1}), and experimental wavenumbers (cm^{-1}) of binary complexes observed upon UV decomposition of GA in argon matrices. The available experimental literature data (cm^{-1}) are shown as well for comparison.

Complex	B3LYPD3/6-311++G(3df,3pd)[1]			Ar matrix this paper	Ar matrix lit. data	Assignment
	ν	I	Δν			
HCHO-H_2O 	3719	90	-20	3706.5, 3703.5sh	3709.3 [31]	$\nu_{as}H_2O$
	3550	207	-98	3569.0	3585.1, 3580.4	$\nu_{s}H_2O$
	2858	62	+58	2884.5	2884, 2879	$\nu_{as}CH_2$
	2781	69	+34	2817.5	2817	$\nu_{s}CH_2$
	1751	95	-17	1735.0	1737	νC=O
	1593	91	+14	1609.5	1610.7	δH_2O
	1486	26	+1	1499.0	1499	δCH_2
	1240	6	+12	1246.0	1245.7	ρCH_2
	1179	6	+12	1173.5	1173.9	τCH_2
HCHO-CO(a) 	2815	104	+13	2823.0		$\nu_{as}CH_2$
	2758	77	+10	2798.5		$\nu_{s}CH_2$
	2162	85	+8	2144.5	2139 [36]	νCO
	1767	119	0	1736.5	1740	νC=O
	1485	12	0	1500.0sh		δCH_2
	1226	10	-2	-		ρCH_2
	1163	4	-5	1171.0		τCH_2
HCHO-CO_2 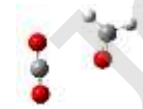	2835	86	+34	2866.0	2867.5 [37]	$\nu_{as}CH_2$
	2768	73	+21	2813.5	2801.8	$\nu_{s}CH_2$
	2344	629	0	2343.0	2341.1	$\nu_{as}CO_2$
	1759	95	-8	1732.5	1737.0	νC=O
	1483	22	-2	1495.5	1495.9	δCH_2
	1233	9	+5	1246.0	1246.0	ρCH_2
	1176	5	+8	1172.5	1169.3	τCH_2
	663	30	+3	666.0[2]	665.9	δCO_2
	646	60	-14	652.5[2]	656.7	δCO_2
H_2O-CO(a) 	3725	125	-14	3726.0, 3720.0[3]	3735.2, 3724.9, 3723.5 [33]	$\nu_{as}H_2O$
	3624	79	-21	3628.5, 3626.5/ 3622.0	3639.4, 3627.8	$\nu_{s}H_2O$
	2169	78	+16	2151.5, 2148.0	2148.2, 2149.2	νCO
	1585	48	+6	1597.0, 1595.0	1599.9, 1595.4	δH_2O

[1] wavenumbers are scaled for anharmonicity by 0.9556 (above 2500 cm^{-1}) and 0.9715 (below 2500 cm^{-1}),
[2] positions of the two most intense bands of a multiple absorption observed in the CO_2 bending region are given,
[3] underlined are those components of the doublets that survived annealing (see text).

Having already identified HCHO-H_2O and H_2O-CO complexes one has to consider formation of the HCHO-CO binary as well as HCHO-CO-H_2O ternary complexes. It is worth noting that Diem *et al.* [36] reported formation of the HCHO-CO "cage" pair formed after photolysis of *trans*-glyoxal in an argon matrix and it was identified based on two bands at 2139 and 1740 cm^{-1}. There is a slight discrepancy between positions of these bands appearing upon glyoxal photolysis and those observed in the present paper. It is most probable due to the presence of the H_2O molecule in the matrix cage upon GA photodecomposition.

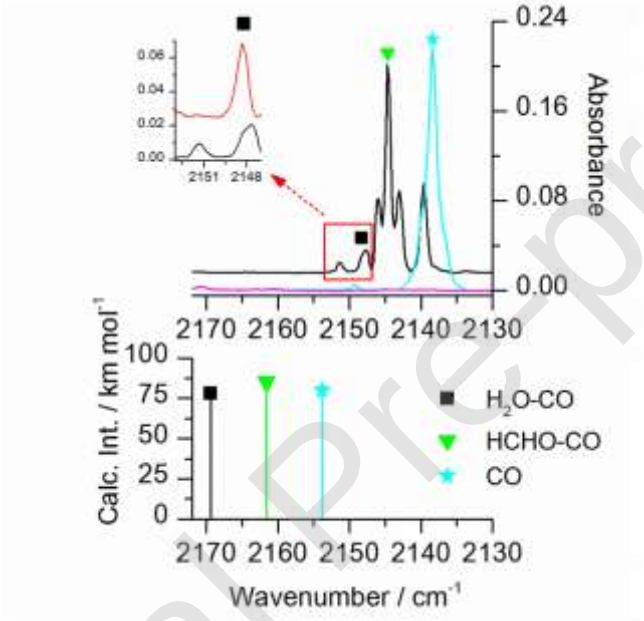

Fig. 3. CO stretching region in the spectra of GA/Ar matrices upon deposition at 15/10K (pink traces) and upon 240 min of irradiation at λ=212 nm (black traces). The inset shows behavior of the H_2O-CO doublet upon 10 min annealing at 30 K/10 K (red trace). CO/Ar=1/1000 spectrum (cyan trace) is presented for comparison. B3LYPD3/6-311++G(3df,3pd) theoretical stick spectra of the species are shown in the bottom of the figure.

As shown in Tables 1 and S2 there are four structures optimized at the B3LYPD3/6-311++G(3df,3pd) level for interaction between HCHO and CO. Only one of them denoted as HCHO-CO(a) is characterized by a positive shift of the CO fundamental of +8 cm^{-1}. This complex has C_{2v} symmetry with the CO subunit attached to CH_2 group of formaldehyde from the carbon end. The most intense band in the νCO region appearing at 2144.5 cm^{-1} with the shift of *ca.* +6 cm^{-1} is a good candidate to be assigned to this binary complex HCHO-CO(a). As shown in Table 1, several other absorptions present in the spectra of irradiated GA/Ar matrices fit relatively well to the theoretical values calculated for formaldehyde modes in the HCHO-CO(a) structure. Among them is a band at 2798.5 cm^{-1} that nearly coincides with the position

reported in the literature for the monomeric formaldehyde [31,32,37] (see Table S1 in Supplementary data). However it must not be assigned to the unbound HCHO due to the weakness of other features expected for this molecule at 2864.1 and 1742.2 cm^{-1}[37].

The origin of the two side bands at 2146.0 and 2143.0 can be due to the HCHO-CO(a) complex located in slightly different matrix sites or can originate from HCHO-CO-H_2O complexes that might appear due to interaction between all three products present in the matrix cage upon photodecomposition of GA. Three such ternary structures differing by relative arrangement of the component molecules have been optimized. The calculated shifts of the νCO mode were found to be +6, +4 and +14 cm^{-1} for HCHO-CO-H_2O(a), HCHO-CO-H_2O(b) and HCHO-CO-H_2O(c), respectively (see Table S3). The experimental shifts relative to the monomeric CO mode [35] are equal to +7.4 and +4.4 cm^{-1}, respectively. Therefore, the presence of such ternary species might not be excluded even though the observed vibrational bands are similar to the H_2O-CO complex. A more distinct study on the ternary complex would be needed in order to scrutinise the spectroscopic difference between the two complex species.

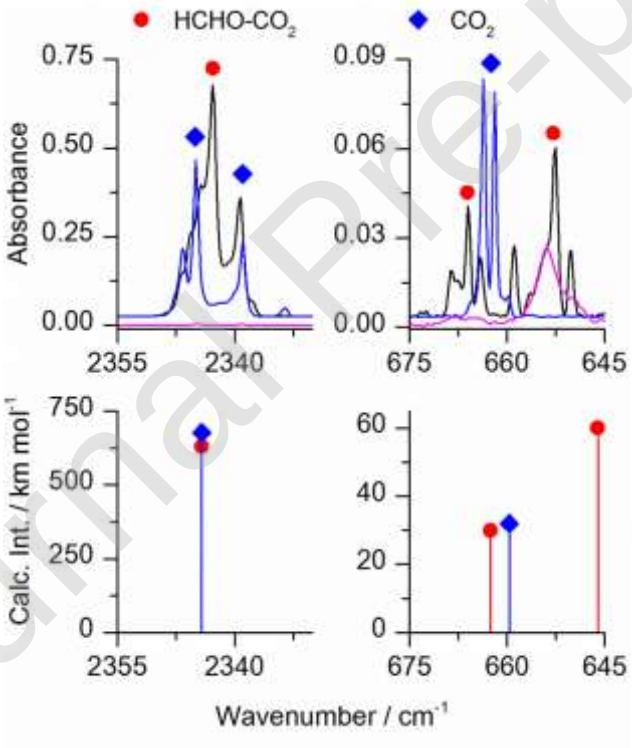

Fig. 4. CO_2 asymmetric stretching and bending regions in the spectra of GA/Ar matrices upon deposition at 15/10K (pink traces) and upon 240 min of irradiation at λ=212 nm (black traces). CO_2/Ar=1/1500 spectrum (blue traces) is shown for comparison. B3LYPD3/6-311++G(3df,3pd) theoretical stick spectra of the species are shown in the bottom of the figure.

Further inspection of the spectra of the irradiated GA/Ar matrices indicates that the CO_2 molecules have to be involved in the photodecomposition processes since, as shown in Fig. 4,

new bands are observed in the vicinity of both stretching and bending modes of carbon dioxide monomer (2345.0/2339.0 and 663.5/662.0 cm^{-1}) (see Table S1) [38]. The first possibility to explain CO_2 presence in the studied matrices would be decarboxylation process of GA leading to CH_3OH and carbon dioxide. However, neither monomeric [39] nor complexed to CO_2 methanol was identified in the spectra upon GA/Ar irradiation. One of the bands appearing upon irradiation in the CO_2 asymmetric stretching region is situated at 2339.5 cm^{-1}. Its position nearly coincides with that observed for pure CO_2/Ar matrix (blue traces in Fig. 4) and as such is assigned to the monomeric CO_2. The same is true for the shoulder at 2344.0 cm^{-1}. The most intense absorption in this region at 2343.0 cm^{-1} fits very well to the position of $\nu_{as}CO_2$ calculated for HCHO-CO_2 complex. Very good agreement between predicted and observed bands position was also found for two bending modes of CO_2 as well as for other spectral regions (see Table 1). Bands due to the HCHO-CO_2 complex are shown as red dots in Figs 2 and 4. It is worth noting that the set of bands observed here is in accord with the one previously reported for this complex by van der Zwet *et al.* [37]. The difference spectrum showing changes upon irradiation at λ=212 nm is presented in Fig. S7 in Supplementary data.

Summarizing, the irradiation of GA/Ar matrices using λ=212 nm leads to photodecomposition of the precursor molecules and formation of four binary complexes: HCHO-H_2O, H_2O-CO, HCHO-CO and HCHO-CO_2. Fig. 5 shows evolution of the absorbance of the selected bands of the above four complexes versus irradiation at 212 nm time.

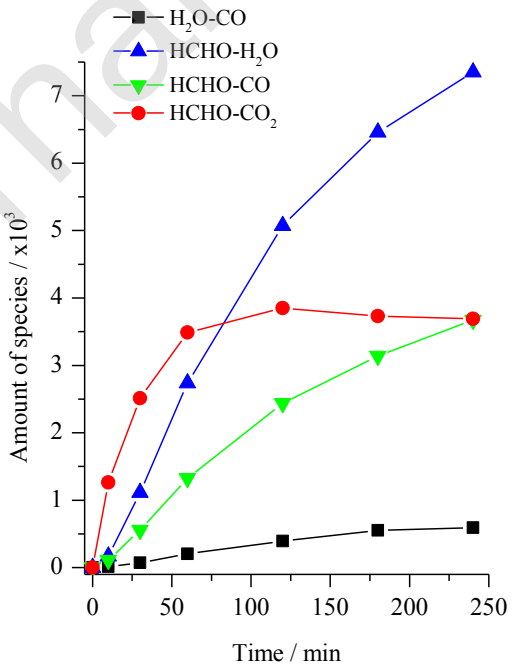

Fig. 5. Kinetic profiles obtained for four binary complexes: H_2O-CO (3726.0/3720.0 cm^{-1}), HCHO-H_2O (3706.5 cm^{-1}), HCHO-CO (2144.5 cm^{-1}) and HCHO-CO_2 (625.5 cm^{-1}) formed upon λ=212 nm irradiation of the GA/Ar matrices. The band used for integration are given in parentheses. In these profiles, the ‘‘amount of species’’ is proportional to the experimental integrated absorbance divided by the calculated infrared intensity of the corresponding vibration.

In plot above “amount of species” is the experimental integrated absorbance divided by the corresponding calculated infrared intensity. Differences in the course of the curves indicate that the products are formed in the matrix with different efficiency. Based on the data presented in Fig. 5, one can make a qualitative difference between the formation of complexes upon UV-photolysis. Most likely the identification of the plethora of complex products is an indication that the UV-induced decomposition of glycolic acid takes place on the excited electronic state instead of ground state, as confirmed by the wavelength used in the experiments (212 nm). The complexes formed indicate that photodecomposition of glycolic acid leads to a radical pair trapped by the matrix medium. The various complexes formed and observed is a demonstration that the radical pair is very short lived and lead to secondary reactions leading eventually to ground state complexes. The different complex structures are also a demonstration that there are different products formed from different glycolic acid isomers. This is in accord with previous reports, for example, on formic acid [33]. However, with the current experimental set-up it is not possible to track down the various radical pairs formed and their reactions pathways in a quantitative way. This would require much faster spectroscopic methods for observation or quantum dynamics simulations to evaluate the chemical processes between ground and excited state potential energy surfaces.

4. Conclusions

Using matrix isolation FTIR spectroscopy and *in situ* narrowband UV irradiation allowed for the first time to establish the main routes of the photolysis of glycolic acid isolated in argon matrices. The presence of the photodecomposition products in the confined volume of the matrix cages led to appearance of different complexes formed between HCHO, H_2O, CO and CO_2. Identification of them was possible based on comparison of the experimental finding with the B3LYPD3/6-311++G(3df,3pd) theoretical infrared spectra and with the relevant literature data. Among these complexes there are four of the 1:1 composition, namely HCHO-H_2O, HCHO-CO, HCHO-CO_2 and H_2O-CO. Monomeric subunits of the complexes are present in small quantities as well.

We believe that the data presented here will help the reader to understand the overall chemical processes taking place and see the complications of having several isomers as a

precursor state for UV photolysis experiments. Also, the observed formation of ground state complexes of stable molecules suggests radical pair formation in the electronic excited state upon photolysis – with subsequent fast reactions and cooling to ground state resulting to molecular complexes.

conflict of interest

There are no conflicts to declare.

Authors contributions

Authors contributions:

Justyna Krupa: Investigation, visualization, editing

Iwona Kosendiak: Investigation,

Maria Wierzejewska: Conceptualization, writing original-draft

Jussi Ahokas: Investigation

Jan Lundell: Conceptualization

Acknowledgment

The research was supported by Academy of Finland Project No. 286844 and 332023 (at JYU). Allocation of computer time from the Wrocław Center for Networking and Supercomputing (Wroclaw, Poland) is gratefully acknowledged.

References

[1] P. D. Godfrey, F. M. Rodgers, R. D. Brown, Theory versus Experiment in Jet Spectroscopy: Glycolic Acid, J. Am. Chem. Soc. 119 (1997) 2232-2239. https://doi.org/10.1021/ja9616793.

[2] D. K. Havey, K. J. Feierabend, V. Vaida, Vapor-Phase Vibrational Spectrum of Glycolic Acid, $CH_2OHCOOH$, in the region 2000-8500 cm^{-1}, J. Phys. Chem. A 108 (2004) 9069-9073. https://doi.org/10.1021/jp0474881.

[3] D. K. Havey, K. J. Feierabend, K. Takahashi, R. T. Skodje, V. Vaida, Experimental and Theoretical Investigation of Vibrational Overtones of Glycolic Acid and Its Hydrogen Bonding Interactions with Water, J. Phys. Chem. A 110 (2006) 6439-6446. https://doi.org/10.1021/jp060602q.

[4] K. Takahashi, K. L. Plath, J. L. Axson, G. C. Nelson, R. T. Skodje, V. Vaida, Dynamics and spectroscopy of vibrational overtone excited glyoxylic acid and 2,2-dihydroxyacetic acid in the gas-phase, J. Chem. Phys. 132 (2010) 094305. https://doi.org/10.1063/1.3327839.

[5] H. Hollenstein, T. K. Ha, H. H. Günthard, IR induced conversion of rotamers, matrix spectra, ab initio

[6] I. D. Reva, S. Jarmelo, L. Lapinski, R. Fausto, First experimental evidence of the third conformer of glycolic acid: combined matrix isolation, FTIR and theoretical study, Chem. Phys. Lett. 389 (2004) 68-74. https://doi.org/10.1016/j.cplett.2004.03.062.

[7] I. D. Reva, S. Jarmelo, L. Lapinski, R. Fausto, IR-induced photoisomerization of glycolic acid isolated in low-temperature inert matrices, J. Phys. Chem. A 108 (2004) 6982-6989. https://doi.org/10.1021/jp0483627.

[8] A. Halasa, L. Lapinski, I. Reva, H. Rostkowska, R. Fausto, M. J. Nowak, Near-infrared laser-induced generation of three rare conformers of glycolic acid, J. Phys. Chem. A 118 (2014) 5626-5635. https://doi.org/10.1021/jp5051589.

[9] J. M. E. Ahokas, I. Kosendiak, J. Krupa, M. Wierzejewska, J. Lundell, High vibrational overtone excitation-induced conformational isomerization of glycolic acid in solid argon matrix, J. Raman Spectr. 49 (2018) 2036-2045. https://doi.org/10.1002/jrs.5474.

[10] C. M. Nunes, I. Reva, R. Fausto, Conformational isomerizations triggered by vibrational excitation of second stretching overtones, Phys. Chem. Chem. Phys. 21 (2019) 24993-25001. https://doi.org/10.1039/C9CP05070A.

[11] A. Nejad, E. Meyer, M. A. Suhm, Glycolic Acid as a Vibrational Anharmonicity Benchmark, J. Phys. Chem. Lett. 11 (2020) 5228-5233. https://doi.org/10.1021/acs.jpclett.0c01462.

[12] I. Kosendiak, J. M. E. Ahokas, J. Krupa, J. Lundell, M. Wierzejewska, Complexes of Glycolic Acid with Nitrogen Isolated in Argon Matrices. I. Structures and Thermal Effects, Molecules 24 (2019) 3262. https://doi.org/10.3390/molecules24183262.

[13] I. Kosendiak, J. M. E. Ahokas, J. Krupa, J. Lundell, M. Wierzejewska, Complexes of Glycolic Acid with Nitrogen Isolated in Argon Matrices. II. Vibrational Overtone Excitations, Molecules 24 (2019) 3245. https://doi.org/10.3390/molecules24183245.

[14] J. M. E. Ahokas, I. Kosendiak, J. Krupa, M. Wierzejewska, J. Lundell, Raman spectroscopy of glycolic acid complexes with N_2, J. Mol. Struct. 1183 (2019) 367-372. https://doi.org/10.1016/j.molstruc.2019.01.080.

[15] I. Kosendiak, J. M. E. Ahokas, J. Krupa, J. Lundell, M. Wierzejewska, FTIR matrix isolation and theretical studies of glycolic acid dimers, J. Mol. Struct. 1163 (2018) 294-299. https://doi.org/10.1016/j.molstruc.2018.03.019.

[16] Z. Moldovan, D. E. Popa, I. G. David, M. Buleandra, I. A. Badea, A Derivative Spectrometric Method for Hydroquinone Determination in the Presence of Kojic Acid, Glycolic Acid, and Ascorbic Acid, J. Spectrosc. 2017 (2017) 6929520. https://doi.org/10.1155/2017/6929520.

[17] Gaussian 16, Revision C.01, M. J. Frisch, G. W. Trucks, H. B. Schlegel, G. E. Scuseria, M. A. Robb, J. R. Cheeseman, G. Scalmani, V. Barone, G. A. Petersson, H. Nakatsuji, X. Li, M. Caricato, A. V. Marenich, J. Bloino, B. G. Janesko, R. Gomperts, B. Mennucci, H. P. Hratchian, J. V. Ortiz, A. F. Izmaylov, J. L. Sonnenberg, D. Williams-Young, F. Ding, F. Lipparini, F. Egidi, J. Goings, B. Peng, A. Petrone, T. Henderson, D. Ranasinghe, V. G. Zakrzewski, J. Gao, N. Rega, G. Zheng, W. Liang, M. Hada, M. Ehara, K. Toyota, R. Fukuda, J. Hasegawa, M. Ishida, T. Nakajima, Y. Honda, O. Kitao, H. Nakai, T. Vreven, K. Throssell, J. A. Montgomery, Jr., J. E. Peralta, F. Ogliaro, M. J. Bearpark, J. J. Heyd, E. N. Brothers, K. N. Kudin, V. N. Staroverov, T. A. Keith, R. Kobayashi, J. Normand, K. Raghavachari, A. P. Rendell, J. C. Burant, S. S. Iyengar, J. Tomasi, M. Cossi, J. M. Millam, M. Klene, C. Adamo, R. Cammi, J. W. Ochterski, R. L. Martin, K. Morokuma, O. Farkas, J. B. Foresman, and D. J. Fox, Gaussian, Inc., Wallingford CT, 2016.

[18] A. D. Becke, Density-functional exchange-energy approximation with correct asymptotic-behavior, Phys. Rev. A 38 (1988) 3098-3100. https://doi.org/10.1103/PhysRevA.38.3098.

[19] A. D. Becke, Density-functional thermochemistry. III. The role of exact exchange, J. Chem. Phys. 98 (1993) 5648-52. https://doi.org/10.1063/1.464913.

[20] C. Lee, W. Yang, R. G. Parr, Development of the Colle-Salvetti correlation-energy formula into a functional of the electron density, Phys. Rev. B 37 (1988) 785-789. https://doi.org/10.1103/PhysRevB.37.785.

[21] S. Grimme, J. Antony, S. Ehrlich, H. Krieg, A consistent and accurate ab initio parameterization of density functional dispersion correction (DFT-D) for the 94 elements H-Pu, J. Chem. Phys. 132 (2010) 154104. https://doi.org/10.1063/1.3382344.

[22] S. Grimme, S. Ehrlich, L. Goerigk, Effect of the damping function in dispersion corrected density functional theory, J. Comp. Chem. 32 (2011) 1456-1465. https://doi.org/10.1002/jcc.21759.

[23] A. D. McLean, G. S. Chandler, Contracted Gaussian-basis sets for molecular calculations. I. Second row atoms, Z=11-18, J. Chem. Phys. 72 (1980) 5639. https://doi.org/10.1063/1.438980.

[24] K. Raghavachari, J. S. Binkley, R. Seeger, J. A. Pople, Self-Consistent Molecular Orbital Methods. XX. Basis set for correlated wave functions, J. Chem. Phys. 72 (1980) 650. https://doi.org/10.1063/1.438955.

[25] S. F. Boys, F. Bernardi, Calculation of small molecular interactions by differences of separate total

[26] S. Simon, M. Duran, J. J. Dannenberg, How does basis set superposition error change the potential surfaces for hydrogen-bonded dimers?, J. Chem. Phys. 105 (1996**)** 11024. https://doi.org/10.1063/1.472902.

[27] D. Licari, A. Baiardi, M. Biczysko, F. Egidi, C. Latouche, V. Barone, Implementation of a graphical user interface for the virtual multifrequency spectrometer: The VMS-Draw tool, J. Comput. Chem. 36 (2015) 321-334. https://doi.org/10.1002/jcc.23785.

[28] R. Bauernschmitt, R. Ahlrichs, Treatment of electronic excitations within the adiabatic approximation of time dependent density functional theory, Chem. Phys. Lett. 256 (1996) 454-464. https://doi.org/10.1016/0009-2614(96)00440-X.

[29] R.E. Stratmann, G.E. Scuseria, M. Frisch, An efficient implementation of time-dependent density-functional theory for the calculation of excitation energies of large molecules, J. Chem. Phys. 109 (1998) 8218-8224. https://doi.org/10.1063/1.477483.

[30] L. R. Domingo, J. Andrés, V. Moliner, V. S. Safont, Theoretical Study of the Gas Phase Decomposition of Glycolic, Lactic, and 2-Hydroxyisobutyric Acids, J. Am. Chem. Soc. 119 (1997) 6415-6422. https://doi.org/10.1021/ja962857v.

[31] B. Nelander, Infrared spectrum of the water formaldehyde complex in solid argon and solid nitrogen, J. Chem. Phys. 72 (1980) 77-84. https://doi.org/10.1063/1.438922.

[32] T. Butscher, F. Duvernay, G. Danger, R. Torro, G. Lucas, Y. Carissan, D. Hagebaum-Reignier, T. Chiavassa, Radical-assisted polymerisation in interstellar ice analogues : formyl radical and polyoxymethylene, Mon. Not. R. Astron. Soc. 486 (2019) 1953-1963. https://doi.org/10.1093/mnras/stz879.

[33] J. Lundell, M. Räsänen, The 193 nm induced photodecomposition of HCOOH in rare gas matrices: the H_2O-CO 1:1 complex, J. Phys. Chem. 99 (1995) 14301-14308. https://doi.org/10.1021/j100039a017.

[34] S. V. Ryazantsev, L. Duarte, V. I. Feldman, L. Khriachtchev, VUV photochemistry of the $H_2O\cdots CO$ complex in noble-gas matrices: formation of the $OH\cdots CO$ complex and the HOCO radical, Phys. Chem. Chem. Phys. 19 (2017) 356-365. https://doi.org/10.1039/C6CP06954A.

[35] H. Dubost, Infrared absorption spectra of carbon monoxide in rare gas matrices, Chem. Phys. 12 (1976) 139-151. https://doi.org/10.1016/0301-0104(76)87051-6.

[36] M. Diem, B. G. MacDonald, E. K. C. Lee, Photolysis and Laser-Excited Fluorescence and Phosphorescence Emission of trans-Glyoxal in an Argon Matrix at 13 K, J. Phys. Chem. 85 (1981) 2227-2232. https://doi.org/10.1021/j150615a018.

[37] G. P. van der Zwet, L. J. Allamandola, F. Baas, J. M. Greenberg, Infrared spectrum of the complex of formaldehyde with carbon dioxide in argon and nitrogen matrices, J. Mol. Struct. 195 (1989) 213-225. https://doi.org/10.1016/0022-2860(89)80170-X.

[38] M. J. Irvine, J. G. Mathieson, A. D. E. Pullin, The infrared matrix isolation spectra of carbondioxide. II Argon matrices: the CO2 monomer bands, Aust. J. Chem. 35 (1982) 1971-1977. https://doi.org/10.1071/CH9821971.

[39] S. W. Han, K. Kim, Infrared matrix isolation study of acetone and methanol in solid argon, J. Phys. Chem. 100 (1996) 17124-17132. https://doi.org/10.1021/jp961538n.Figure Caption

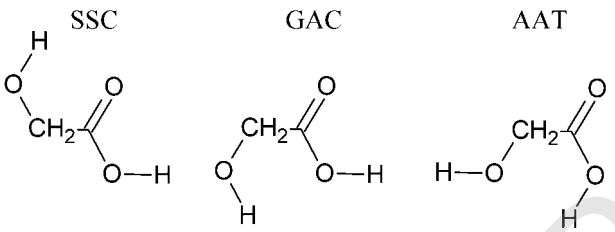

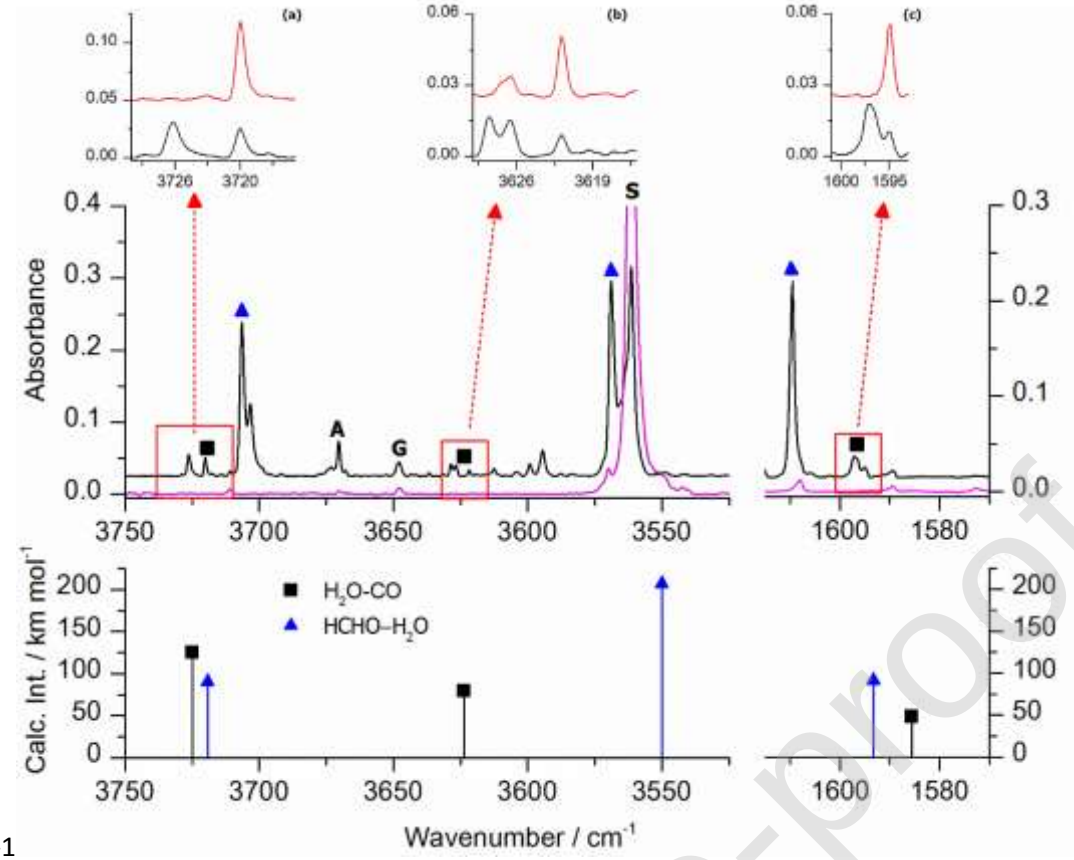

Figr-1

Figr-2

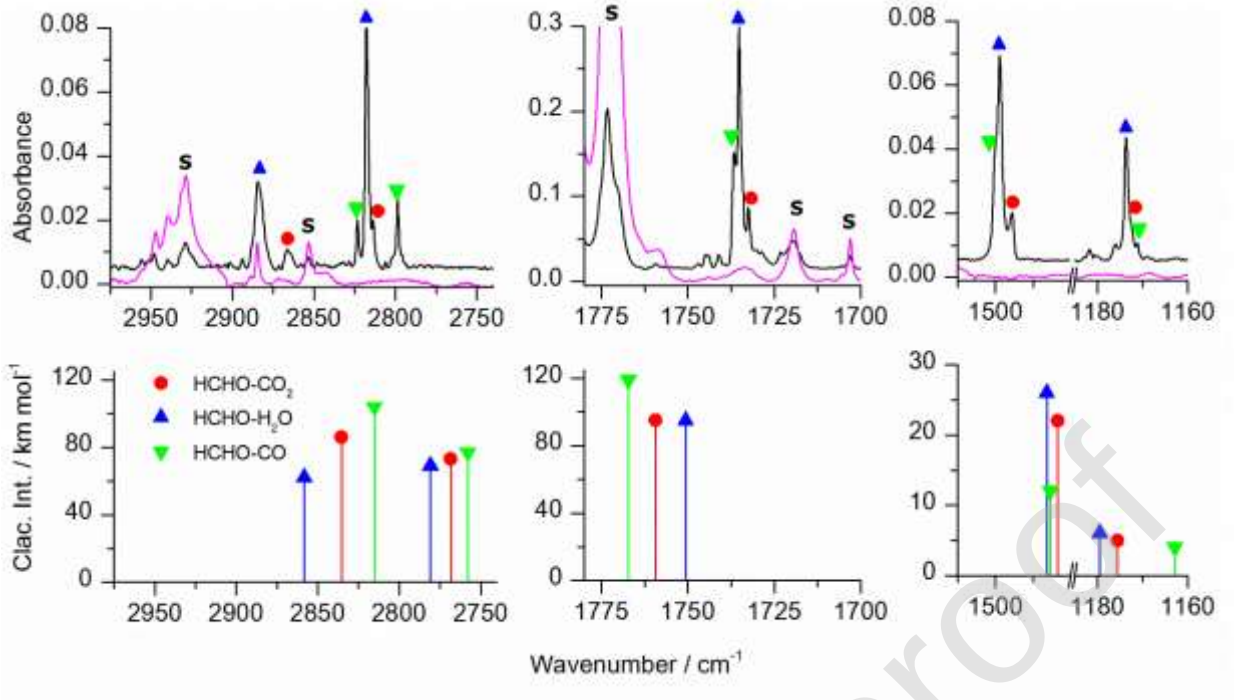

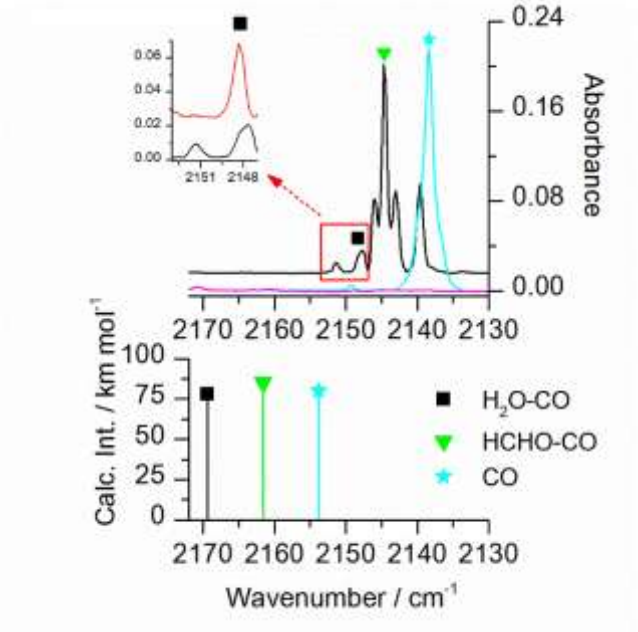

Figr-3

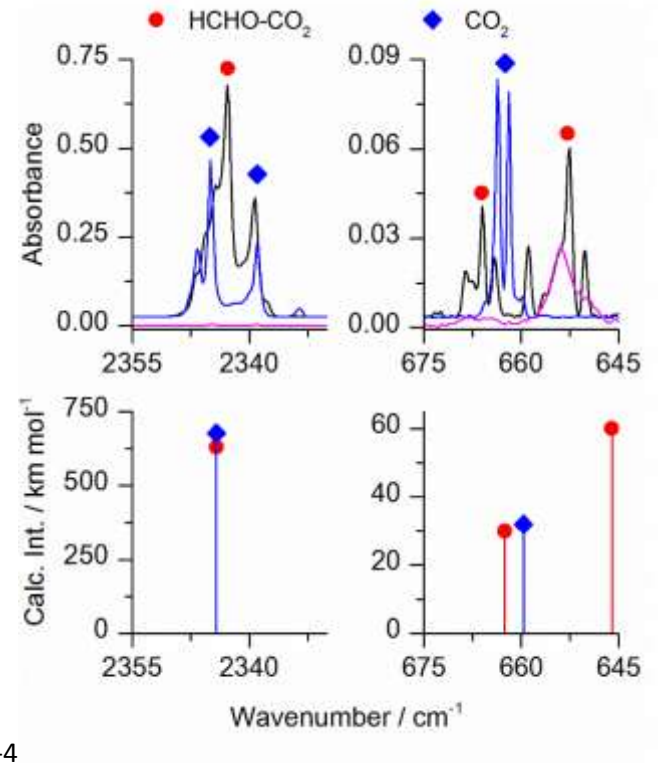

Figr-4

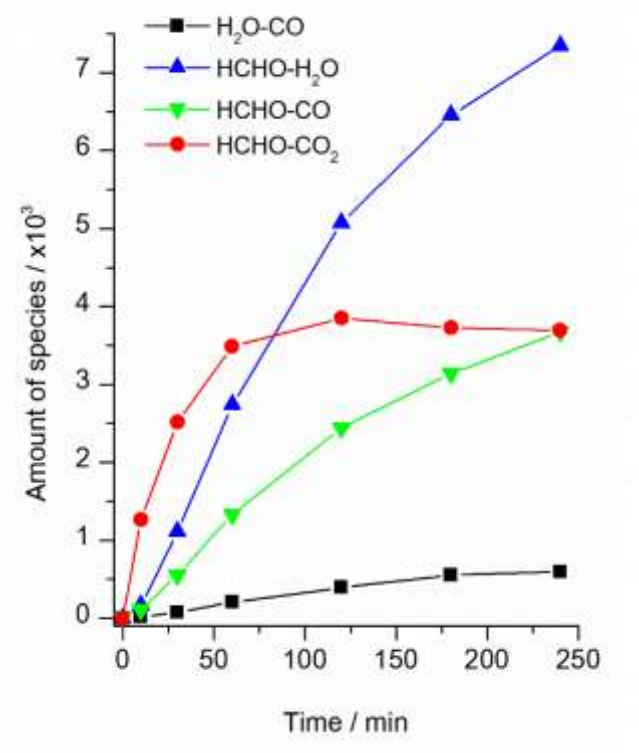

Figr-5

Figr-8**Figure captions**

Scheme 1. Schematic representation of three most stable conformers of glycolic acid monomer.

Fig. 1. Water asymmetric and symmetric stretching and deformation regions in the spectra of GA/Ar matrices upon deposition at 15/10K (pink traces) and upon 240 min of irradiation at λ=212 nm (black traces). The insets show behavior of the H_2O-CO doublets upon 10 min annealing at 30 K/10 K (red traces). B3LYPD3/6-311++G(3df,3pd) theoretical stick spectra of HCHO-H_2O and H_2O-CO are shown in the bottom of the figure. Letters A, G and S denote AAT, GAC and SSC conformers of glycolic acid, respectively.

Fig. 2. Selected regions of HCHO complexes with H_2O, CO and CO_2 in the spectra of GA/Ar matrices upon deposition at 15/10K (pink traces) and upon 240 min of irradiation at λ=212 nm (black traces). B3LYPD3/6-311++G(3df,3pd) theoretical stick spectra of the complexes are shown in the bottom of the figure. Letter S denotes SSC conformer of glycolic acid.

Fig. 3. CO stretching region in the spectra of GA/Ar matrices upon deposition at 15/10K (pink traces) and upon 240 min of irradiation at λ=212 nm (black traces). The inset shows behavior of the H_2O-CO doublet upon 10 min annealing at 30 K/10 K (red trace). CO/Ar=1/1000 spectrum (cyan trace) is presented for comparison. B3LYPD3/6-311++G(3df,3pd) theoretical stick spectra of the species are shown in the bottom of the figure.

Fig. 4. CO_2 asymmetric stretching and bending regions in the spectra of GA/Ar matrices upon deposition at 15/10K (pink traces) and upon 240 min of irradiation at λ=212 nm (black traces). CO_2/Ar=1/1500 spectrum (blue traces) is shown for comparison. B3LYPD3/6-311++G(3df,3pd) theoretical stick spectra of the species are shown in the bottom of the figure.

Fig. 5. Kinetic profiles obtained for four binary complexes: H_2O-CO (3726.0/3720.0 cm^{-1}), HCHO-H_2O (3706.5 cm^{-1}), HCHO-CO (2144.5 cm^{-1}) and HCHO-CO_2 (625.5 cm^{-1}) formed upon λ=212 nm irradiation of the GA/Ar matrices. The band used for integration are given in parentheses. In these profiles, the ‘‘amount of species’’ is proportional to the experimental integrated absorbance divided by the calculated infrared intensity of the corresponding vibration.

Table 1. Calculated and scaled harmonic wavenumbers ν (cm^{-1}), intensities I (km mol^{-1}) and shifts relative to the corresponding monomers Δν (cm^{-1}), and experimental wavenumbers (cm^{-1}) of binary complexes observed upon UV decomposition of GA in argon matrices. The available experimental literature data (cm^{-1}) are shown as well for comparison.

Complex	B3LYPD3/6-311++G(3df,3pd)[1]			Ar matrix this paper	Ar matrix lit. data	Assignment
	ν	I	Δν			
HCHO-H_2O 	3719	90	-20	3706.5, 3703.5sh	3709.3 [31]	$\nu_{as}H_2O$
	3550	207	-98	3569.0	3585.1, 3580.4	$\nu_{s}H_2O$
	2858	62	+58	2884.5	2884, 2879	$\nu_{as}CH_2$
	2781	69	+34	2817.5	2817	$\nu_{s}CH_2$
	1751	95	-17	1735.0	1737	νC=O
	1593	91	+14	1609.5	1610.7	δH_2O
	1486	26	+1	1499.0	1499	δCH_2
	1240	6	+12	1246.0	1245.7	ρCH_2
	1179	6	+12	1173.5	1173.9	τCH_2
HCHO-CO(a) 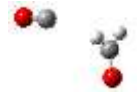	2815	104	+13	2823.0		$\nu_{as}CH_2$
	2758	77	+10	2798.5		$\nu_{s}CH_2$
	2162	85	+8	2144.5	2139 [36]	νCO
	1767	119	0	1736.5	1740	νC=O
	1485	12	0	1500.0sh		δCH_2
	1226	10	-2	-		ρCH_2
	1163	4	-5	1171.0		τCH_2
HCHO-CO_2 	2835	86	+34	2866.0	2867.5 [37]	$\nu_{as}CH_2$
	2768	73	+21	2813.5	2801.8	$\nu_{s}CH_2$
	2344	629	0	2343.0	2341.1	$\nu_{as}CO_2$
	1759	95	-8	1732.5	1737.0	νC=O
	1483	22	-2	1495.5	1495.9	δCH_2
	1233	9	+5	1246.0	1246.0	ρCH_2
	1176	5	+8	1172.5	1169.3	τCH_2
	663	30	+3	666.0[2]	665.9	δCO_2
	646	60	-14	652.5[2]	656.7	δCO_2
H_2O-CO(a) 	3725	125	-14	3726.0, <u>3720.0</u>[3]	3735.2, <u>3724.9, 3723.5</u> [33]	$\nu_{as}H_2O$
	3624	79	-21	3628.5, <u>3626.5/ 3622.0</u>	3639.4, <u>3627.8</u>	$\nu_{s}H_2O$
	2169	78	+16	2151.5, <u>2148.0</u>	2148.2, <u>2149.2</u>	νCO
	1585	48	+6	1597.0, <u>1595.0</u>	1599.9, <u>1595.4</u>	δH_2O

[1] wavenumbers are scaled for anharmonicity by 0.9556 (above 2500 cm^{-1}) and 0.9715 (below 2500 cm^{-1}),
[2] positions of the two most intense bands of a multiple absorption observed in the CO_2 bending region are given,
[3] underlined are those components of the doublets that survived annealing (see text).